Applied Physics Express

LETTERS

Thermal characterization of microscale heat convection in rare-gas environment by a steady-state “hot wire” method

Applied Physics Express **11**, 066601 (2018)
https://doi.org/**10.7567/APEX.11.066601**

Thermal characterization of microscale heat convection in rare-gas environment by a steady-state "hot wire" method

Jianshu Gao[1,2], Danmei Xie[1,2], Yangheng Xiong[1,2], and Yanan Yue[1,2,3*]

[1]*Key Laboratory of Hydraulic Machinery Transients (Wuhan University), MOE, Wuhan 430072, China*
[2]*School of Power and Mechanical Engineering, Wuhan University, Wuhan 430072, China*
[3]*Department of Mechanical Engineering, Boston University, Boston, MA 02215, U.S.A.*

*E-mail: yyue@whu.edu.cn

Received January 31, 2018; accepted April 13, 2018; published online May 10, 2018

In this work, a steady-state "hot wire" method is developed to study thermal transport around a microwire in a rare-gas environment. The convection heat transfer coefficient (h) around a 25 μm platinum wire is determined to be from 14 W m^{-2} K^{-1} at 7 Pa to 629 W m^{-2} K^{-1} at atmospheric pressure. In the free-molecule regime, the Nusselt number is found to be inversely proportional to the Knudsen number, the slope of which is used to determine the slip length as 7.03×10^{-4} m. In the transition regime, the slip length is found to be 20 times the wire diameter. Under a certain pressure, h decreases with increasing wire temperature, and this trend is more sensitive at high pressures.

Thermal management at the microscale has become a crucial issue as the dimension of electronics continues to scale down with enhanced power density.[1)] Much attention has been focused on the enhancement of the heat conduction property of solids,[2,3)] while ignoring the convective thermal transport process at such a scale. Indeed, for materials at the micro/nanoscale, the characteristic length in convection is comparable to the mean free path of gas molecules. The heat convection between gas molecules and a hot surface is of equal importance,[4)] and somehow can be regarded similarly to the heat conduction performance. It has been experimentally confirmed that the convection heat transfer coefficient (h) at the microscale is several orders of magnitude larger than that of the bulk material.[5)] To date, quantitative analyses for comprehensively understanding heat dissipation involving conduction, convection, and radiation effects at the microscale are still insufficient due to the lack of thermal characterization technologies. In particular, for some extreme conditions such as rare-gas environments, thermal characterization is even more challenging while such knowledge is increasingly required for engineering needs.

The heat convection effect highly depends on the buoyancy force driven by the temperature difference and the viscosity of gas. However, since the buoyancy force is negligible when the sample size shrinks to the micro/nanoscale in a rare-gas environment,[6)] heat convection is indeed dominated by heat conduction between gas molecules and a hot surface. Convection heat loss around a material at the micro/nanoscale is strongly related to the characteristic length of the material and the mean free path of gas molecules. The flow regime is classified into the following four types as a function of Knudsen number (the radio of the mean free path of molecules to the characteristic length):[7)] the continuum regime ($Kn < 0.01$), slip regime ($0.01 < Kn < 0.1$), transition regime ($0.1 < Kn < 10$), and free-molecule regime ($Kn > 10$). In the free-molecule regime, the gas density is small so the gas molecules hardly collide with each other. Convection heat loss is ascribed to the collisions between gas molecules and a hot surface.[8)]

In the past, Cheng et al. reported convection heat loss around wires with different diameters at various pressures.[9)] h is sensitive to pressure when the pressure is lower than 13 Pa. When the pressure is more than 10^4 Pa, the sample diameter has a greater influence on h. Wang et al. proposed a model for h prediction between a carbon nanotube and gas environment which is valid for both the free-molecule regime and continuum regime.[10)] h at the microscale has been demonstrated to be several orders of magnitude larger than that at the macroscale.[11)] The increase of the surface to volume ratio was considered as the main contributor to the enhancement of heat convection at the microscale. In addition, h varied by several orders of magnitude for different heater sizes even though all of them were fabricated in nanoscale thin-film structures.[12)]

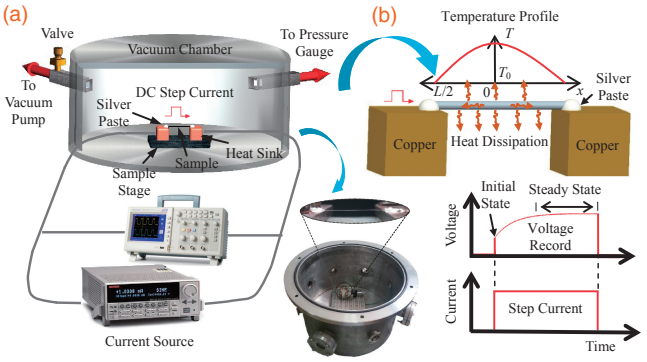

Fig. 1. (a) Schematic and optical image for measuring convective heat transfer coefficient in rare-gas environment. (b) Heat dissipation inside the wire through heat conduction, heat convection from wire surface to surrounding air, and heat radiation. The voltage variation of the wire during the heating process is used to obtain the wire temperature.

In this work, we present a method to characterize thermal transport around a microwire in a rare-gas environment by using a steady-state "hot wire" method. h is obtained under various rare-gas conditions. The slip length is also obtained, which reflects the distance of thermal influence for a certain diameter of wire. This term is determined in both the free-molecule regime and transition regime to analyze how heat carriers diffuse and collide with each other, which is meaningful for the thermal design of micro/nanoelectronics.

A wire is suspended between two heat sinks in a steel chamber as shown in Fig. 1(a). Joule heating introduced by DC step current is generated inside the sample and dissipates through axial conduction heat loss, convection heat loss, and radiation heat loss to determine the temperature profile along

the wire, which can be expressed as $\partial^2 T/\partial x^2 + (Q - Q_{air})/kA_cL = 0$, where T is the local temperature along the wire, x is the distance away from the sample middle point, k is the thermal conductivity, Q is the Joule heating power, A_c is the cross-section area of the sample, and L is the length. The term Q_{air} is the convection heat loss and is described as $Q_{air} = h_e PL(T - T_0)$, where P is the cross-section perimeter of the wire, T_0 is room temperature, and h_e is the effective convection heat transfer coefficient (combining the effects of heat convection and radiation). Assuming that the sample ends stay at room temperature, the average temperature rise of the wire is calculated as

$$\Delta\bar{T} = \frac{Q}{h_e LP} - \frac{2Q}{h_e L^2 P\sqrt{h_e P/kA_c}} \tanh\left(\frac{L\sqrt{h_e P/kA_c}}{2}\right). \quad (1)$$

After subtracting the radiation heat loss, h is obtained as $h = h_e - \varepsilon\sigma(\bar{T}^4 - T_0^4)/(\bar{T} - T_0)$, where ε is the emissivity (0.05 for the platinum wire)[13] and σ is the Stefan-Boltzmann constant. We choose a wire material with its electrical resistance very sensitive to temperature. The wire itself is employed as a temperature sensor so that the voltage variation recorded during the heating process can provide temperature information.[14] When the wire is heated under different DC step currents at various pressures, h can be obtained from the average temperature rise of the wire with a constant thermal conductivity.

This steady-state "hot wire" method shares a similar experimental setup to the conventional hot wire method but has a different measurement principle.[15] The conventional hot wire method is based on a transient thermal transport process, and heat conduction along the wire is not considered. Actually, the temperature profile along the wire is not uniform; thus, heat conduction, heat convection, and heat radiation are all involved. In our method, heat conduction along the wire is taken into account.

The platinum wire (above 99.95% purity from manufacturer) used in this experiment has a diameter of 25 μm and length of 19.44 mm. Platinum wire possesses very stable thermal conductivity (71.6 $W m^{-1} K^{-1}$) for temperatures from 73 to 1273 K.[16] The wire is suspended between two large copper electrodes with its ends firmly attached by silver paste to reduce contact resistance. The copper electrodes are used as heat sinks due to the large thermal conductivity and heat capacity. Thus, the assumption that the sample ends stay at room temperature in the physical model is reasonable.[17,18] Even there is a little temperature rise or there is another heat dissipation effect induced by the sample end, such effects can be considered in the data processing to reduce the uncertainty.[19,20] The pressure in the chamber is controlled by a valve from 7 Pa to atmospheric pressure. The steel chamber is much larger than the sample to ensure a constant temperature for the chamber in the measurement. The wire is heated under different DC step currents (Keithley 6220) from 10 to 86 mA. The voltage signal is recorded by a data acquisition card (NI USB-6003).

We firstly calculated h and then calculated the different types of heat loss in the heat convection process. Axial conduction heat loss (Q_{cond}) is larger than convection heat loss (Q_{conv}) for pressures lower than 10 Pa ($Q_{cond}/Q_{conv} > 1$) as shown in Fig. 2(a). When the microwire is heated by a power of 1.866 mW in air at 7 Pa, Q_{cond} is 1.2 times Q_{conv} with $\Delta\bar{T}$

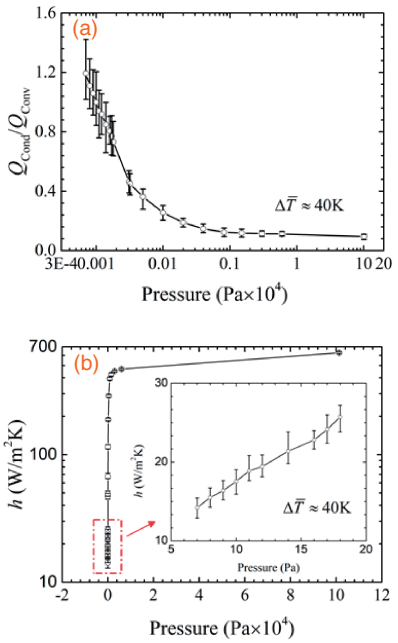

Fig. 2. (a) Ratio of conduction to convection heat loss for different pressures. (b) h with respect to pressure at a constant temperature rise. The inset shows the linearly increasing trend of h with pressure.

of the wire around 40 K. As the pressure is increased, heat is dissipated more through convection. It is found that Q_{cond} along the wire cannot be neglected since it still accounts for 9% of the convection heat loss at atmospheric pressure, which confirms our prerequisite that heat conduction along the wire still matters. Figure 2(b) shows h as a function of pressure when $\Delta\bar{T}$ of the wire is around 40 K. h varies from 14 $W m^{-2} K^{-1}$ (7 Pa) to 629 $W m^{-2} K^{-1}$ (atmospheric pressure), which is in good agreement with reference results.[21] In a rare-gas environment, the buoyancy force is not significant so that h determined in this work is valid for a microwire placed in different orientations.[22]

It is found that h firstly experiences a rapid increase at lower pressures, and then a slower increase toward atmospheric pressure. There is a transition point around 28 Pa. Below this point, h increases rapidly with pressure and thermal transport is defined as ballistic thermal transport. That means gas molecules have little chance to collide with each other after reflecting from the hot wire. When the pressure is higher than 28 Pa, heat convection is gradually dominated by diffusion thermal transport.

Since the wire temperature is determined by the voltage variation during the heating process, the uncertainty of h is mainly contributed to the noise in the voltage signal. Each voltage signal is repeatedly measured multiple times then averaged to minimize uncertainty. The thermal conductivity of the platinum wire remains constant during the heating process. When the thermal conductivity is changed within the highest level (say 5%), the corresponding maximum relative uncertainty of h is around 9% at our lowest pressure and 0.26% at atmospheric pressure. In the measurement, it is highly recommended to use a stable wire as the temperature sensor, especially in low-pressure measurement. Schiffres and Malen employed a metal-coated SiO_2 wire with lower thermal conductivity than that of a pure metallic wire to reduce heat conduction along the wire. Then, it was much

easier to characterize the heat convection effect of the wire in low-pressure measurement.[23] However, it is assumed in our measurement that the thermal conductivity of the wire is very stable in the case that the variation of k during the heating process leads to large uncertainties in determining h. The metal-coated wire might be unsuitable for fulfilling such a requirement.

In addition, h obtained in this measurement is an averaged value along the wire. It is noticeable that the selection of a suitable wire length is important for characterizing the local h on the wire. A long wire means heat convection and heat radiation accounts for a larger proportion of heat dissipation and the effect of contact resistance may be neglected. However, a larger difference occurs when characterizing the local h with the average h in our mode because the temperature difference along the wire is enlarged. The fluid around the wire can be changed into other liquids or rare gases. For materials with unknown thermal conductivities, we can first obtain the thermal property of a solid wire and its temperature dependence in vacuum.[24] Then h under different heating powers and pressures can be obtained using our technique.

The ballistic thermal transport, characterized by the Nusselt number in the free-molecule regime, is introduced as[25]

$$Nu_{\text{free}} = \left[\frac{1}{\alpha_1} + \left(\frac{D_1}{D_2}\right)\left(\frac{1}{\alpha_2} - 1\right)\right]^{-1} \frac{(\gamma+1)}{Kn(9\gamma-5)}\sqrt{\frac{T_{\text{m,DF}}}{T_{\text{m,FM}}}}, \tag{2}$$

where α_1 is the thermal accommodation coefficient at a hot surface (0.87 for the air molecule-platinum interaction),[26] α_2 is the thermal accommodation coefficient at a natural convection boundary, D_1 is the wire diameter, D_2 is the slip length, γ is the specific heat ratio (1.4 for the air molecules), $T_{\text{m,DF}}$ is the effective mean temperature used to calculate Kn, and $T_{\text{m,FM}}$ is the effective temperature of the air. In the calculation of the Knudsen number ($Kn = \lambda/D_1$), the mean free path of gas molecules (λ) is defined as $\lambda = k_B T_{\text{m,DF}}/(\sqrt{2}\pi d^2 P)$,[27] where k_B is the Boltzmann constant, d is the air molecular diameter (3.72×10^{-10} m[28]), and P is the gas pressure in the chamber. If the temperature rise of the wire is small, there is not much difference between $T_{\text{m,DF}}$ and $T_{\text{m,FM}}$, and the value can be defined as the average temperature of the wire and environment.

Since h_{free} is closely related to Nu_{free} ($Nu = hD_1/k_{\text{air}}$), D_2 in the free-molecule regime can be derived from h_{free} based on Eq. (2). As demonstrated in Fig. 3(a), h_{free} decreases as Kn is increased in the free-molecule regime. Kn reveals the degree of rarefaction in a flow.[29] As Kn becomes infinitely large ($1/Kn$ approaches zero), the density of air molecules is infinitely small and there is no convection heat transfer. The theoretical curve based on Eq. (2) remains a constant smaller than the characterized h_{free}. In Fig. 3(b), Nu_{free} is sensitive to the inverse Knudsen number ($1/Kn$) in the free-molecule regime. From Eq. (2), Nu_{free} is a linear function of $1/Kn$, which means that the intercept of the linear fitting for Nu_{free} versus $1/Kn$ should be zero. However, the intercept of the linear fitting for Nu_{free} versus $1/Kn$ is determined as 0.007. The nonzero value of the intercept is from the contact at the sample ends. Specifically, the contact points have some electrical resistance even if silver paste is employed to attach the sample ends to the heat sinks. The total Joule heating

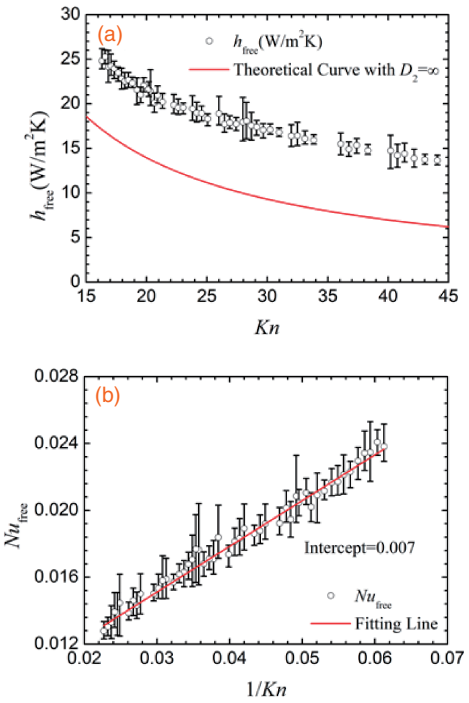

Fig. 3. (a) h_{free} as a function of Kn in free-molecule regime, compared with theoretical curve obtained based on Eq. (2). (b) Relationship between Nu_{free} and $1/Kn$ in the free-molecule regime. The intercept of the fitting line (red line) for Nu_{free} versus $1/Kn$ is determined as 0.007, which can be used in data correction.

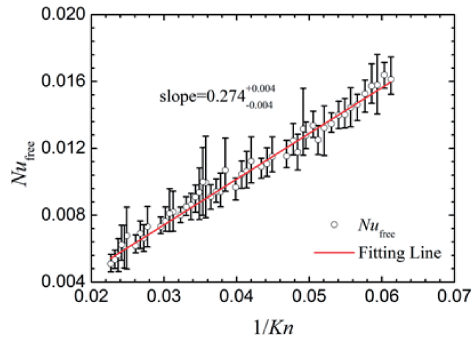

Fig. 4. Values of Nu_{free} after correction as a function of $1/Kn$ in the free-molecule regime.

is included in the calculation while only the temperature rise of the wire is used for deriving h_{free}. Both the additional heating effect from the contact resistance and the interaction at the hot surface of the contact points with air molecules affect the measurement results, and lead to the overestimated value of h_{free}. By subtracting the constant value of the intercept, the values of the Nusselt number can be corrected based on the intercept of the fitting line in Fig. 3(b).

The values of Nu_{free} after correction are shown in Fig. 4. In the free-molecule regime, heat is transferred by single collisions between gas molecules and the hot wire surface. Thermal transport is sensitive to $1/Kn$ with a fitted slope of 0.274 ± 0.0040. By using an accommodation coefficient of 0.92 for the steel-air interaction,[28] the slip length of the transport process is determined as 7.03×10^{-4} m based on Eq. (2). It means that the effect of heat dissipation in the free-molecule regime is from the hot wire and extends to a

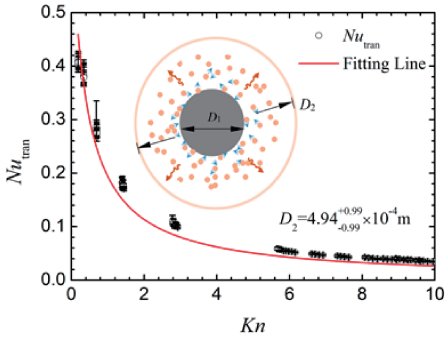

Fig. 5. Value of Nu_{tran} under various Kn in transition regime. A theoretical prediction based on Eq. (3) is introduced to calculate the slip length in the transition regime by fitting the experimental data.

distance of almost 30 times the wire diameter. Similar free-molecule convection has been observed in other studies. For example, Hsu et al. compared different heat dissipation paths of individual single-walled carbon nanotube (CNT) bundles in vacuum and air environments.[30] The convection heat transfer coefficient was determined to be in the range from 1.5×10^3 to $7.9 \times 10^4\,\mathrm{W\,m^{-2}\,K^{-1}}$. Considering that the diameter of our sample (25 μm) is far larger than that of their CNTs (9.89–12.9 nm), our characterization result (around $600\,\mathrm{W\,m^{-2}\,K^{-1}}$ in air) is reasonable. Another work by Schiffres et al. reported that the length scale of thermal transport from collisions between gas molecules and CNTs could be two hundreds of magnitude larger than the size of the pores in CNT aerogels, which is an important reason for the extremely small thermal conductivity as characterized in the experiment.[31]

In the transition regime, the heat dissipation process is dominated by both ballistic thermal transport and diffusion thermal transport. Heat convection through the collision of gas molecules is described as[32]

$$Nu_{\mathrm{tran}} = \left[1 + \alpha_1 \frac{4B}{15}\frac{1}{2Kn}\ln\left(\frac{D_2}{D_1}\right)\right]^{-1} Nu_{\mathrm{free}}, \qquad (3)$$

where $B = 1.184$ for a diatomic gas. As shown in Fig. 5, the value of Nu_{tran} is decreased with increasing Kn. By comparison with the theoretical curve (red line in Fig. 5), the slip length is determined as $(4.94 \pm 0.99) \times 10^{-4}$ m, which is around 20 times the wire diameter. In the transition regime, diffusion thermal transport plays a significant role. Gas molecules which reflect from the wire collide with other gas molecules. The intermolecular collisions result in a smaller Nu_{tran} in the transition regime than that obtained through ballistic thermal transport.[33] As Kn becomes smaller, the distinction between them is more significant, which well explains why the enhancement of thermal transport by molecules is more significant in the free-molecule regime than in the transition regime.

Temperature is another factor that significantly influences heat convection.[34] The value of h under different wire temperatures is shown in Fig. 6(a). It is found that as the pressure is varied from 7 to 200 Pa, the value of h is decreased with increasing wire temperature. Although the buoyancy force is neglected in heat convection at the micro/nanoscale, the wire temperature affects the rate of heat transfer between the hot surface and gas molecules by changing the density and

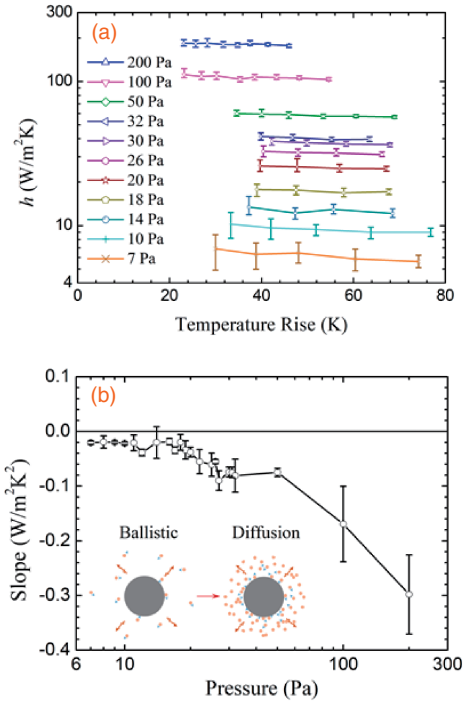

Fig. 6. (a) Effect of wire temperature on h at different pressures. (b) Slopes of h versus temperature from free-molecule regime to transition regime.

kinetic energy of gas molecules around the hot wire.[35] In Fig. 6(b), the slopes of h versus temperature are drawn under different pressures with the 95% confidence interval in the fitting process. It shows that the slope experiences a continuous decrease as pressure is increased. It can be understood that a higher temperature gives a larger Kn when pressure is fixed, and thus weakens the heat convection effect. When thermal transport evolves from ballistic thermal transport to diffusion thermal transport (pressure is increased), such an effect (the response of the heat transfer performance to temperature) is more significant.

In summary, the value of h of a microwire under different heating and pressures is characterized by using a steady-state hot wire method. Different from the conventional hot wire technique, our proposed method considers the heat conduction and heat convection as well as the heat radiation effect along the wire. By employing a platinum wire as the wire cylinder and a temperature sensor, we have successfully characterized the heat transfer performance around a microwire from the free-molecule regime to transition regime. It is found that Nu shows a linear relationship with $1/Kn$ in the free-molecule regime. The slip length is also obtained in both the free-molecule regime and transition regime, which can be used for analyzing the thermal influence zone around a hotspot when designing nanoelectronics. We also found that at a certain pressure, h decreases with increasing temperature and that the slope of h versus temperature experiences a continuous decrease as pressure is increased.

Acknowledgments The financial support from the National Natural Science Foundation of China (No. 51576145) is gratefully acknowledged.

1) S. Kaur, N. Raravikar, B. A. Helms, R. Prasher, and D. F. Ogletree, Nat. Commun. **5**, 3082 (2014).
2) Y. N. Yue, J. C. Zhang, X. D. Tang, S. Xu, and X. W. Wang, Nanotechnol. Rev. **4**, 533 (2015).

3) Y. Yue, J. Zhang, Y. Xie, W. Chen, and X. Wang, Int. J. Heat Mass Transf. **110**, 827 (2017).
4) J. Zhang, E. Strelcov, and A. Kolmakov, Nanotechnology **24**, 444009 (2013).
5) J. Doll, E. Corbin, W. King, and B. Pruitt, Appl. Phys. Lett. **98**, 223103 (2011).
6) Z.-Y. Guo and Z.-X. Li, Int. J. Heat Fluid Flow **24**, 284 (2003).
7) N. Dongari and A. Agrawal, Int. J. Heat Mass Transf. **55**, 4352 (2012).
8) M. Darbandi and E. Roohi, Int. Commun. Heat Mass Transf. **38**, 1443 (2011).
9) C. Cheng, W. Fan, J. B. Cao, S. G. Ryu, J. Ji, C. Grigoropoulos, and J. Q. Wu, ACS Nano **5**, 10102 (2011).
10) H.-D. Wang, J.-H. Liu, X. Zhang, T.-Y. Li, R.-F. Zhang, and F. Wei, J. Nanomater. **2013**, 181543 (2013).
11) Z. L. Wang and D. W. Tang, Int. J. Therm. Sci. **64**, 145 (2013).
12) R. A. Pulavarthy, M. T. Alam, and M. A. Haque, Int. Commun. Heat Mass Transf. **52**, 56 (2014).
13) C. H. Xing, C. Jensen, T. Munro, B. White, H. Ban, and M. Chirtoc, Appl. Therm. Eng. **73**, 317 (2014).
14) X. Wan, C. Li, Y. Yue, D. Xie, M. Xue, and N. Hu, Nanotechnology **27**, 445706 (2016).
15) J. Lee, H. Lee, Y. J. Baik, and J. Koo, Int. J. Heat Mass Transf. **89**, 116 (2015).
16) S. Azarfar, S. Movahedirad, A. Sarbanha, R. Norouzbeigi, and B. Beigzadeh, Appl. Therm. Eng. **105**, 142 (2016).
17) M. Li and Y. Yue, J. Nanosci. Nanotechnol. **15**, 3004 (2015).
18) Y. Yue, K. Liu, M. Li, and X. Hu, Carbon **77**, 973 (2014).
19) Y. Yue, G. Eres, X. Wang, and L. Guo, Appl. Phys. A **97**, 19 (2009).
20) Y. Yue, X. Huang, and X. Wang, Phys. Lett. A **374**, 4144 (2010).
21) P. Liu, Z. Fan, A. Mikhalchan, T. Q. Tran, D. Jewell, H. M. Duong, and A. M. Marconnet, ACS Appl. Mater. Interfaces **8**, 17461 (2016).
22) C. Silvestri, M. Riccio, R. Poelma, B. Morana, S. Vollebregt, F. Santagata, A. Irace, G. Q. Zhang, and P. Sarro, Nanoscale **8**, 8266 (2016).
23) S. Schiffres and J. Malen, Rev. Sci. Instrum. **82**, 064903 (2011).
24) J. Q. Guo, X. W. Wang, and T. Wang, J. Appl. Phys. **101**, 063537 (2007).
25) E. H. Kennard, *Kinetic Theory of Gases with an Introduction to Statistical Mechanics* (McGraw-Hill, New York, 1938).
26) L. Gottesdiener, J. Phys. E **13**, 908 (1980).
27) X. L. Zhang, L. Z. Xiao, X. W. Shan, and L. Guo, Sci. Rep. **4**, 4843 (2014).
28) Z. M. Zhang, *Nano/Microscale Heat Transfer* (McGraw-Hill, New York, 2007).
29) V. K. Michalis, A. N. Kalarakis, E. D. Skouras, and V. N. Burganos, Microfluid. Nanofluid. **9**, 847 (2010).
30) I. K. Hsu, M. Pettes, M. Aykol, C.-C. Chang, W.-H. Hung, J. Theiss, L. Shi, and S. Cronin, J. Appl. Phys. **110**, 044328 (2011).
31) S. Schiffres, K. Kim, L. Hu, A. J. H. McGaughey, M. Islam, and J. Malen, Adv. Funct. Mater. **22**, 5251 (2012).
32) Y. Demirel and S. C. Saxena, Energy **21**, 99 (1996).
33) H. H. Klein, J. Karni, R. Ben-Zvi, and R. Bertocchi, Sol. Energy **81**, 1227 (2007).
34) M. Li, C. Z. Li, J. M. Wang, X. H. Xiao, and Y. N. Yue, Appl. Phys. Lett. **106**, 253108 (2015).
35) M. T. Alam, A. P. Raghu, M. A. Haque, C. Muratore, and A. A. Voevodin, Int. J. Therm. Sci. **73**, 1 (2013).